Static Real Time Localisation with a collinear time of flight (TOF) sonar triplet

Willibroad ABONGWA ACHO[1]* Klaus SCHILLING[2], Radu BARZA[3], Wolfgang NZIE[4]
[1&4] Department of Mechanical Engineering, ENSAI, The University of Ngaoundere - BP 455, Ngaoundere, Cameroon
[2&3] *Autonomous Robotics Systems (ARS) Lab. (2002-2003 academic year)*
The University of Applied Sciences Ravensburg – Weingarten, Germany.

ABSTRACT

It is well known that the sonar return of the monaural time of flight (TOF) sonar sensor is characterised by a wide noise margin. This investigation was therefore aimed at developing a sonar sensor model based on the monaural model which could localize more precisely and instantly *or in real-time* at least, a *point target* in an *unknown* 2D space. Experimenting with different microcontroller driven transducer configurations and echo modes lead to the formulation of this *proposition*: A collinear monaural sonar triplet operating in the multiple echo mode offers ample opportunity for the development of an embedded software for the instant localization of a *point target.* Accordingly, an embedded software named a *geometric filter* was developed and implemented thus producing an intelligent TOF *sonar ranging triplet.* A localization test with the triplet highlighted an error bound of 0.0 to - 2.5cm and 0.0 to 8.5cm in the X and Y direction of the horizontal plane of the triplet respectively. When the localization software was reviewed, it was possible to localize point targets with a precision of less than 2.5cm, thus, supporting our proposition. In addition, this study hypothesizes that the epicentre of reflected sound energy does not always coincide spatially with the initiating point.

Key words: monaural model, real time localization, sensor model, intelligent TOF sonar ranging triplet, point target, geometric filter.

RÉSUME

Les recherches ont déjà montré que le retour sonar du type temps de vol monaural est caractérisé par une marge d'erreur importante. Cette recherche a eu pour objectif de modéliser un capteur basé sur le modèle monaural qui pouffait localiser plus précisément et immédiatement ou en temps réel, un point cible dans un espace 2D inconnu. L'expérience avec différentes configurations de capteurs et modes d'écho conduite par un microcontrôleur a conduit à la formulation de cette proposition: un triplet des capteurs monauraux et alignées, fonctionnant en mode multiple échos offre une opportunité de développement d'un logiciel intégré pour une localisation instantanée d'un point cible. En conséquence, un logiciel intégré appelé filtre géométrique a été réalisé, produisant ainsi un triplet sonar intelligent du type temps de vol. Un test de localisation avec ce triplet montre une marge d'erreur de 0,0 à 2,5 cm et de 0,0 à 8,5 cm respectivement dans les sens X et Y du plan horizontal du triplet. Quand le logiciel de localisation a été passé en revue, il a été possible de localiser des point cibles avec une précision de moins de 2,5 cm, confirmant ainsi notre proposition. En outre, l'hypothèse de cette étude est que l'épicentre de la réflexion de l'énergie sonore ne coïncide pas toujours dans l'espace avec le point qui l'initie.

Mots clés: modèle monaural, localisation en temps réel, modéliser un capteur, triplet sonar intelligent du type temps de vol, point cible, filtre géométrique

* **Corresponding Author**

1. INTRODUCTION

The time-of-flight sonar sensors*(referred to throughout this text as TOF sonars)* have so far enjoyed enormous popularity amongst sensor experts and mobile robot enthusiasts because of its simplicity and low cost. It has been used with various degrees of success for obstacle avoidance and navigation of mobile robots in a mapped 2D space. Its main drawback remains its relatively poor ranging capabilities. This is because the simplest form of a TOF sonar sensor in which the ultrasonic transducer functions both as a transmitter and a receiver of ultrasonic energy is plagued with the following problems:-

1. Data association problem due to the wide visibility angle. In other words, the origin of a sonar return can at best be any point on a circular arc defined by a radius equal to the sonar return and the visibility angle.

2. Cross-talk when two or more sensors are used.

3. Weak energy returns and poor hardware timing can introduce significant errors.

4. A specula target may not be seen if it is not properly oriented.

For these reasons, it has been pretty difficult to use the monaural sonar for precise and instant or *real time* localization of any point on a target in 2D space. Expectedly, the point in question should correspond to the epicentre of reflected ultrasonic energy and it is what is referred to throughout this text as a *point target.* Evidently, the problem of localizing an object in an unknown 2D space will become even more tractable if point targets are precisely localize.

As faras localization in 2D space with the monaural sonar is concerned, some outstanding efforts have been made[1],[2]. However, the methods proposed by these authors, generally require a considerable amount of *a priori* data collection and processing before any point can be localized. The scale of data collection and processing prescribed is usually not practicable on a small mobile robot whose computational capacity is normally limited by that of it's on-board micro-controllers. Other schemes such as those proposed Leornard and Durant Whyte [3], and Wijk and Christensen [4] are applicable only to what is generally referred to as localization of a previously mapped terrain. Another important contribution tackled the issue of localization with

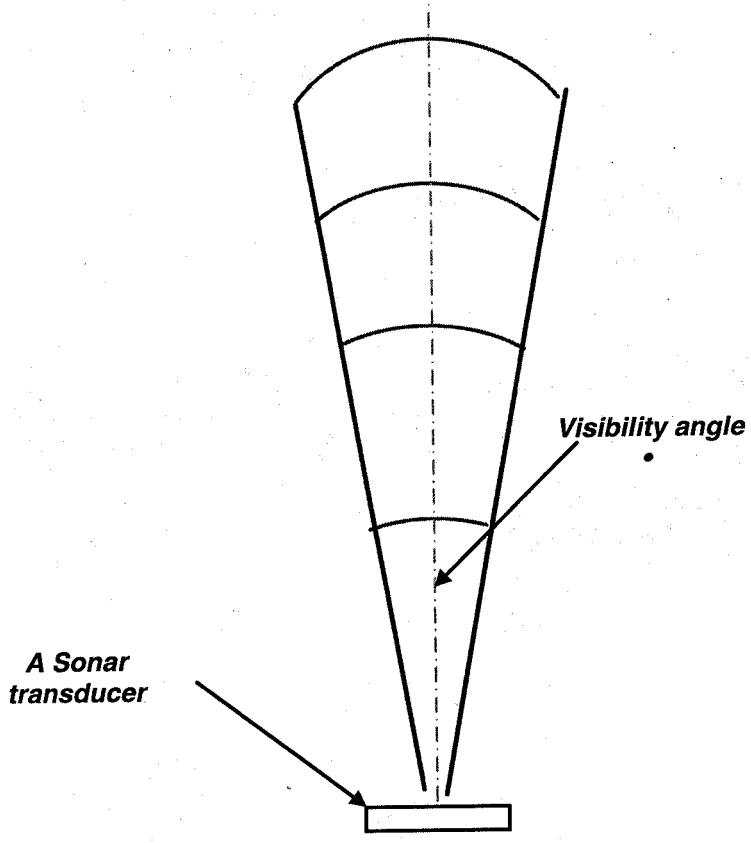

Fig 1.1 . The simple beam (or monaural) TOF sonar model

a monaural sonar from the point of view of building up an *occupancy grid map* [4] which is usually associated with a bulky localization code[6]. None of these systems can localize a point (the *simplest geometric object*) in 2D space within a fraction of a second or instantly if the terrain in question had not been previously mapped. In other words, these systems can not be implemented on a mobile robot that has to perform autonomous navigation tasks in unknown environments. No doubt, so many important efforts have been made towards localization with the time of flight sonar that are not strictly speaking based on the monaural model. As such, it has not been found necessary to review them.

It is for this reason that it was found necessary to investigate the capacity of the simplest form of the *TOF* sonar (the monaural sonar) to localize a point in 2D space with a precision relevant to the navigation of a small mobile robot in an unmapped 2D terrain. Specifically, therefore, this investigation was aimed at developing a *TOF* sonar system based on the monaural model (Fig.1.1) that is capable of localizing instantly or in *real time* a point (or *more precisely a point target)* in 2D space. Naturally, the static performance of the system envisaged has to be to be assessed for a start. It is expected that this effort would contribute to the problem of real time localization or autonomous navigation in 2D space of small mobile robots equipped with only the monaural TOF sonars as on-board external ranging sensors.

2. MATERIALS AND METHODS

The ranging and obstacle avoidance facilities on the *MERLIN (Mobile Experimental Robots for Locomotion and Intelligent Navigation)* rovers of the ARS lab, the University of Applied Science, Weingarten - Germany, were used for this investigation. The Merlin rovers are car-like mobile robots (Fig 2.1) each having four *monaural* sonar transducers (three in front and one at the rear) that are energized by the Polaroid® 6500 module. The Polaroid module is designed to operate one or more monaural sonar transducer units. The operation of the module is controlled by an Infineon™ 167CR-LM micro-controller via relays. In other words, the sonar system in question is operated by an embedded software. The original system developer is PHYTEC™ ***Messtechnik GmbH***, Germany.

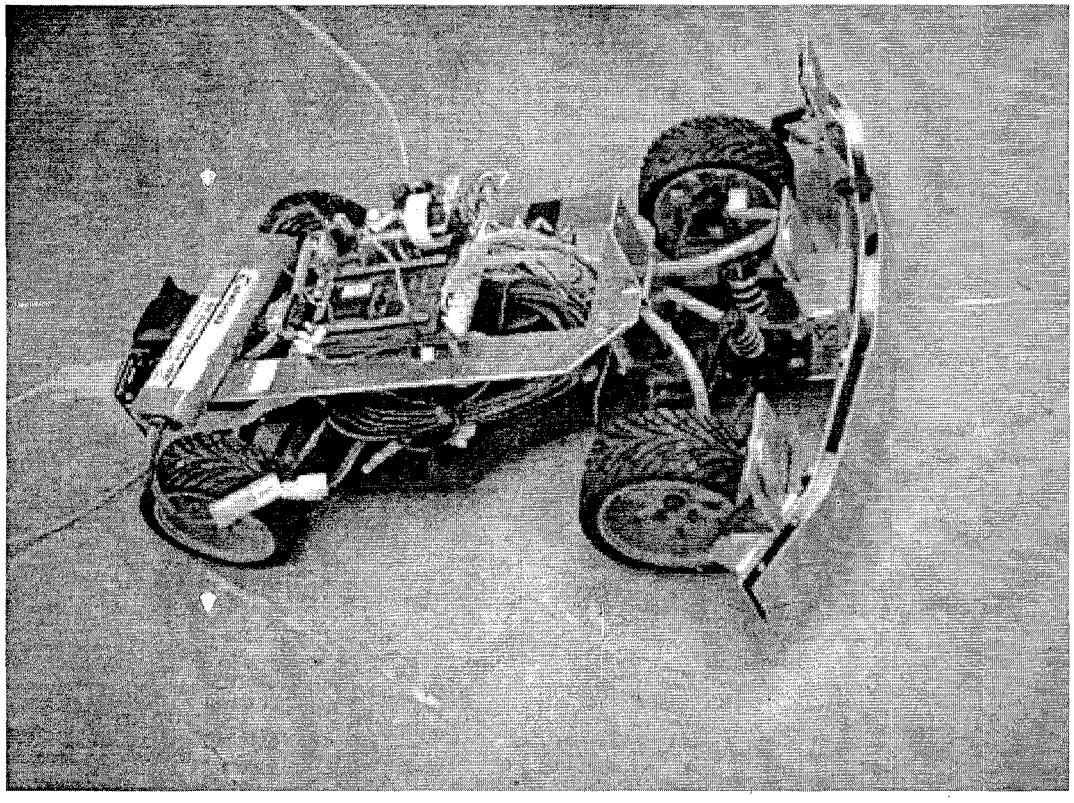

Fig. 2.1 . The MERLIN Rover of the ARS Lab , The University of Applied Sciences, Weingarten Germany.

2.1 Programming the Merlin's sonar module for multiple echo operation.

The next issue that had to be tackled was related to the following questions: How many monaural transducers should be used (using just one has obviously not been successful so far)? What should be the spatial configuration of the transducers? Are there possibilities of incorporating an embedded software to improve the efficiency of ranging? It was therefore obvious that some preliminary investigations had to be done to observe the sonar return data when two or three sonar transducers are operating firstly, in the single echo mode and secondly, in the multiple echo mode using arbitral targets. These investigations revealed that the sonar return pattern is related to the geometry of the target. It was also observed that a sizeable amount of sonar return data can be generated when the module is operating in the multiple echo mode. The size of this data was judged to be quite handy in the sense that it can be used as code data for an embedded software that could provide a better picture of the nature and range of a target within few seconds. Hence, it was decided that the sonar transducers on-board the MERLIN should be programmed for multiple echo reception. Thereafter, a localization algorithm would have to be developed after carefully studying the data pattern generated by the multiple echo system. Another preliminary investigation also indicated that the visibility angle $\hat{a}$, of each transducer used was approximately 20°. This value lies within the range of 15 and 30° as reported in earlier investigations. What actually limits the visibility angle is definitely a subject for further investigation.

An explanation of the operation the Polaroid Module is freely available on the net. So it is just sufficient to state here that each of the four transducers was programmed to receive four echoes before switching on to the next after every 325ms. The controller had an embedded code to compute the range of a target. The code was also capable of discrimination targets that were 11cm apart. Theoretically, the minimum possible discrimination between two targets associated with the Polaroid system in question is just below 8cm but we settled for 11cm because a preliminary investigation indicated that above this value the discriminated values were more consistent and accurate for perpendicular targets. The time interval between two switching actions allowed for a maximum range of about 552 cm for each transducer.

2.2 Ranging experiments and observations

In other to develop a localization code, it was necessary to conduct some localization tests with simple geometric objects and study the data emanating thereof. First of all, the transducers in front of the Merlin were aligned so as to make them perpendicular to the centreline of the robot, (see Fig. 2.2a and 2.2b). A length of 14.5 cm was adopted as the distance between the two transducers. Thereafter, range measurements were taken for the following targets: two specula planes - one of them inclined, a concave and then a convex surface, both with a radius of curvature of 15cm, and finally an approximate point target represented by a cylinder of diameter 15mm (see Fig. 2.3). In experiment (e), a rectangular target had its two edges roughened with sand paper. The data collected for each of these situations are displayed in Appendix A.

After a careful study of the data issuing from these experiments, it was evident that the targets could be classified as follows: -

- *Point Targets- seen by at least, two transducers:* These are edges or objects of length of at least 7mm – the approximate wavelength of the ultrasonic radiation in operation. Because of the relatively small spatial separation of the transducers, an edge is in-

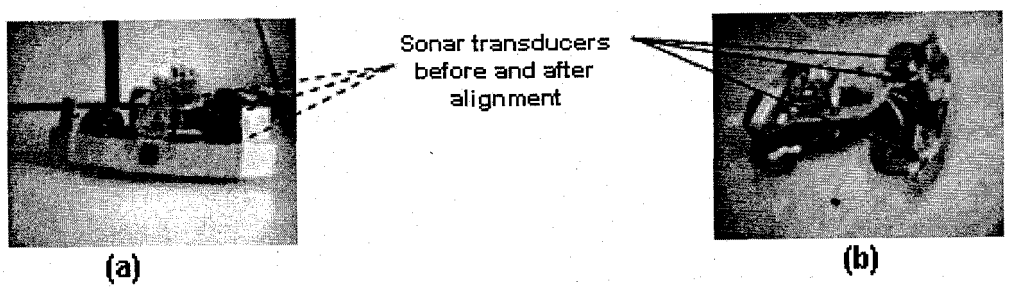

Fig. 2.2. The sonar transducers in front of the Merlin before (a), and after (b) alignment

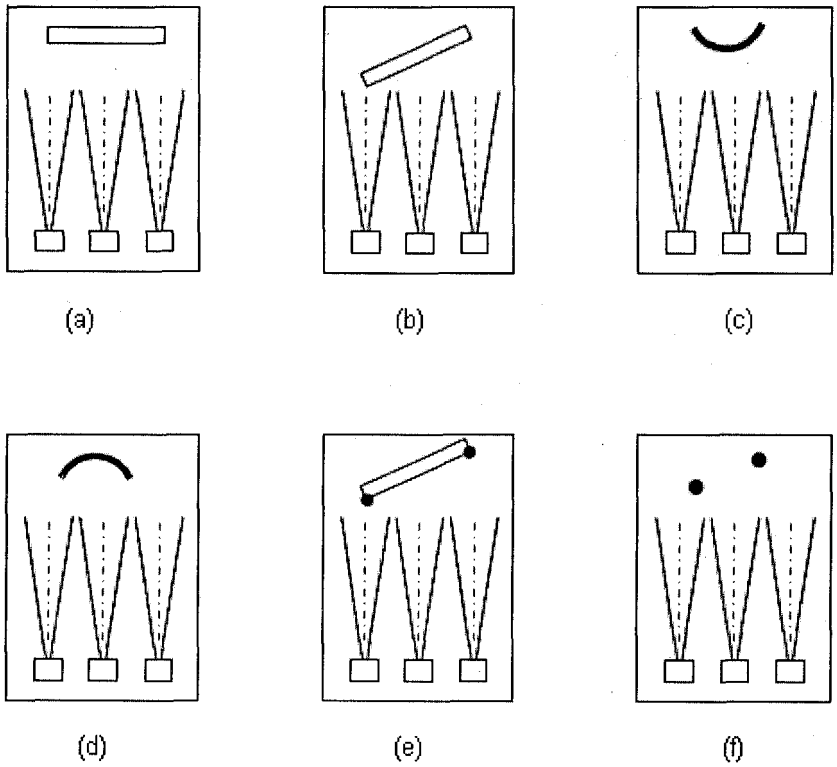

Fig. 2.3. Graphical Representations of the tests conducted with the Sonar triplet.

dicated by the closeness in value of either the first or second sonar return detected by two adjacent transducers. An extract of the data recorded for experiment (f) is shown in Fig. 2.4. We can observe a correspondence between the second return of the first transducer and the first return recorded by the second transducer, i.e. 185 and 182cm respectively. We can also suspect another correspondence between 229 and 236 cm. It must be emphasized however, that if a correspondence is observed we must not rush to conclude that an edge or a point target has been seen. For example (Fig 2.4 b), 201 and 202 are close enough but there are chances that this data pair may not be emanating from the same point since the two transducers are quite close to each other and the second return of transducer 1(*Sen1Tag1*) is less than the first return of transducer 2 (Sen2Tag1).

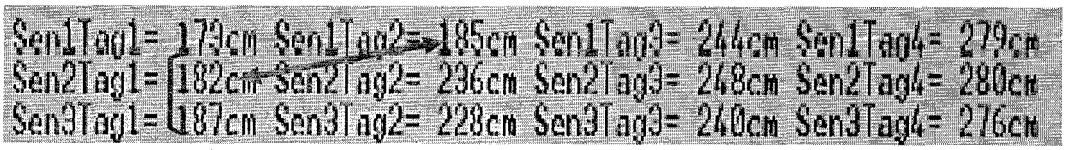

a) Typical data from Experiment (f).

b) Typical data from. Experiment (e).

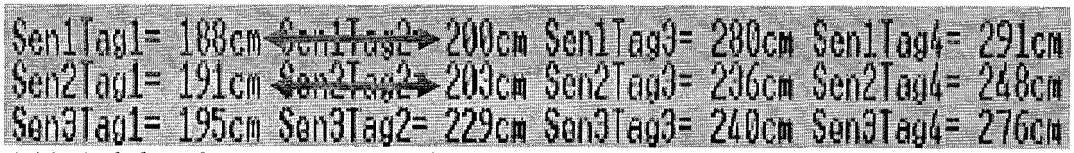

c) Typical data from Experiment (d).

Fig. 2.4. Data Extracted from Appendix A

• *Perpendicular Plane Target:* Expectedly, it was observed that if a perpendicular plane target is located symmetrically within the field of view of the three transducers, at least two sonar returns are always equal and a third sonar return is also always equal to the others or at most 1.0 cm more.

• *Convex surface:* The data recorded for a convex surface was very similar to that recorded for a plane. This may be due to rounding since the data was "floored" in code, or the fact the two sensors at the edges of the triplet may have picked up returns from side lobs or weak signals which are error prone. This abnormality may also be traced to inherent alignment problems of the system that was used.

• *Concave surface:* Characteristically, the transducer at the middle of the triplet always recorded a second return which is about the minimum discrimination more than the first return.(see Fig. 2.4c). This can be explained by the fact that multiple reflections are possible and at least two successive echoes can be generated. This makes the detection of concave surfaces relatively easier.

What has been observed so far suggests that as long as a *point target* is within the view of at least two transducers of the triplets, a data correspondence would appear as illustrated in Fig. 2.4 thus providing us with a candidate point target that can be localized in 2D space. This assertion, assumes that the returning echoes are both of high and approximately equal energy because of reasons advanced in section 1. A candidate point target identified as such can be localized(determining it's x, y coordinates) in 2D space by *triangulation.* To do this, the two transducers in question and the *point target* must be associated with a rectangular frame of reference as shown in Fig. 2.5. In this Figure, r1 and r2 are the range values detected by sonar transducer 1 (T1) and transducer 2 (T2) respectively. Point P is any point target and d is the distance between the transducers. Accordingly, the following equations are valid :

$$Cos\phi_1 = \frac{1}{2r_2 d}\left(r_2^2 + d^2 - r_1^2\right) \quad \text{.....(2.1}$$

$$Cos(\phi_2) = \frac{1}{2r_1 d}\left(r_1^2 + d^2 - r_2^2\right) \quad \text{.....(2.2}$$

Hence the coordinate of the point target will be given by

$$P(x, y) = \left(r_1 Cos\phi_1 , r_2 Sin\phi_2\right) \quad \text{.....(2.3}$$

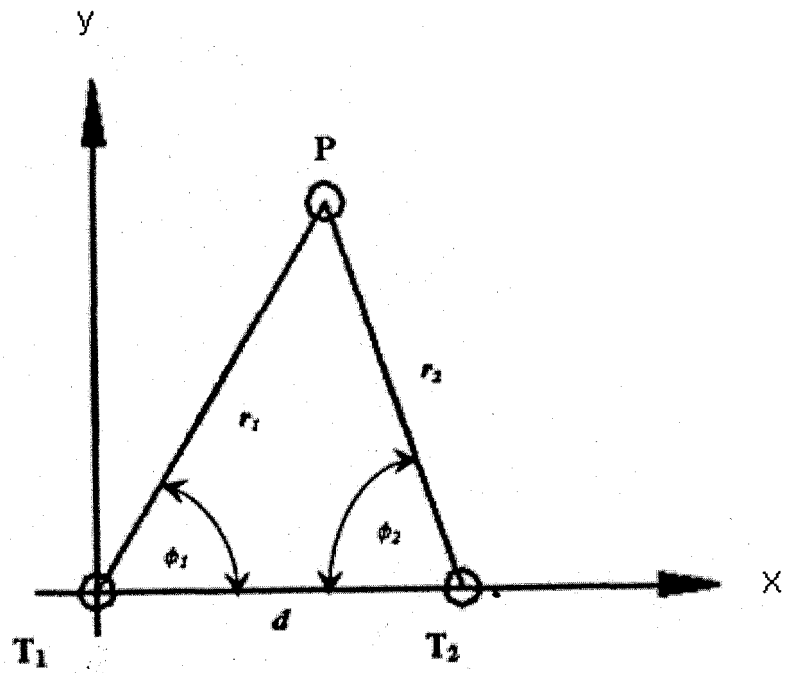

Fig. 2.5 Triangulation method to determine the coordinates of a Point Target, P

Theoretically, a point target localized this way, would be relatively less erroneous compared with the localisation of a single monaural transducer. We can confirm the validity of a position localized by triangulation by verifying whether it lies within the sonar visibility angle $\hat{a}$, of any of the two transducers in question - that is;

$$90 - \phi_{1 \text{ or } 2} \leq \tfrac{1}{2}\beta \quad \ldots\ldots\ldots\ldots\ldots\ldots \quad (2.4$$

If the data of experiments (b) and (e) are compared we also realize that the sand paper made the edges more "visible" because not a single data correspondence was observed in experiment (b) but we observed a correspondence between 229 and 236 as shown by Fig 2.4b. This suggests that the edges of the target can be made to be "sonar friendly" either by sticking sandpaper or thin cylinders of at least, 7mm on its edges. Done this way, the edges are always going to be "seen" even if the surface between the edges can not be seen because of its orientation.

In a nutshell, we can conclude that the data from a collinear TOF sonar triplet can be used to localize at least, a point target. This lead to the formulation of the following proposition: The sensor model illustrated geometrically by Fig. 2.6 can be used to localize a point target if converted into an embedded software. It consists of three equally spaced collinear transducers. Attached to this model is a mobile rectangular reference frame originating from the mid-point of the leftmost transducer (A). This model also assumes an imaginary limit (define by the width of view) within which a point target can be localized by the method illustrated by Fig. 2.5. Furthermore any sonar return not found between the minimum and maximum possible return of the triplet will be considered not to have been "seen". The minimum and maximum return should be determined a priori and systematically implemented in software. Eventually, it is also expected that this model would be capable of recognising and localizing planes as well as concave and convex short profiles with cord length less the width of view. Since an embedded signal processing and filtering algorithm is envisaged this model has been given the name, *The Intelligent TOF Sonar Ranging Triplet Sensor Model.* The distance between a pair of transducers is indicated as D_T. in Fig 2.6.

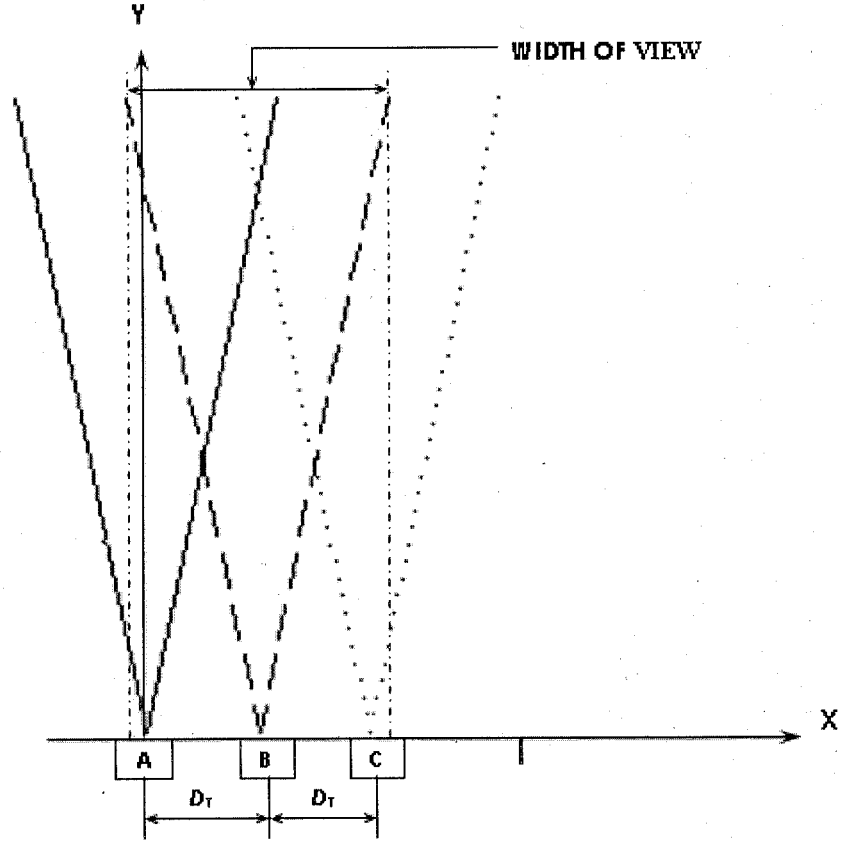

Fig 2.6. Geometric Model of the Intelligent TOF Sonar Ranging Triplet Sensor

3. IMPLEMENTING THE INTELLIGENT TOF SONAR RANGING TRIPLET SENSOR MODEL

3.1 Localization Algorithm for the TOF Sonar Intelligent Ranging Triplet

The next logical task of this investigation was to attempt an implementation of the Intelligent TOF Sonar Ranging Triplet sensor model thus obtaining what may be named as a **Intelligent TOF Sonar Ranging Triplet** . The implementation of this model should permit the localization of a point target. As indicated in the previous section, localization in this case simply means getting the X and Y coordinates of a point target. This was in effect, a task that consisted of developing and implementing an algorithm *(as an embedded software)* that selects and then confirms *candidate point targets*, using equations 2.1 through 2.4. Accordingly, the three sonar transducers in front of the Merlin rover and associated electronic modules constituted our sonar triplet system. The distance between each pair of transducers of the triplet was maintained at 14.5cm. The width of view as defined by the sensor model illustrated by Fig. 2.6 was also conveniently chosen to be 29cm.

The candidate point selection module of the localisation code was based primarily on the "geometric" logic table illustrated in Fig. 3.1. Two adjacent transducers can "*see*" two point targets in any of the eight possible scenarios depending on the visibility angle, the distance between each point target and the transducers, the distance between the points and the spatial separation of the transducers. A single transducer will not be able to discriminate between two point targets within its view if the distance between them is less than the minimum discrimination, which in this case, is 11cm. However, if another target or another epicentre of reflected energy is 11cm beyond the first, this would be indicated by another return of 11cm greater than the first.

A pair of return was considered to have originated from a candidate point if its absolute difference is a value *considerably* less than the precision we seek to achieve. From the same figure, the following situations are obvious: -

- The first sonar return recorded by both transducers, **A** and **B,** suggests a candidate point (cases illustrated by 1, 2, 4, 8).
- The first sonar return recorded by transducers **A** and the second return by **B** suggests a candidate point (illustrated by 3).
- The second sonar return recorded by transducers **A** and the first return recorded by **B** suggests a candidate point (illustrated by 6).
- The sonar returns recorded by both transducers are from two different point targets (illustrated by 5). In this case, the algorithm will detect no second return for both transducers.
- The two transducers records the same value of their respective first *and second* sonar returns. This should happened if the target is perpendicular to the axis of the sensor (illustrated by 7).

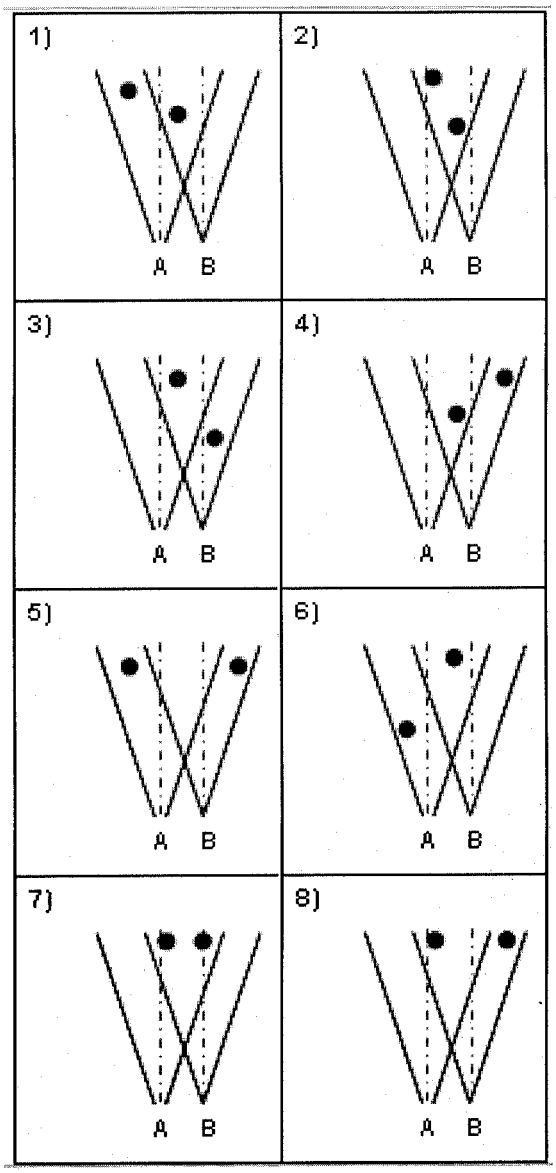

Fig. 3.1. Eight possible view configurations of two point targets

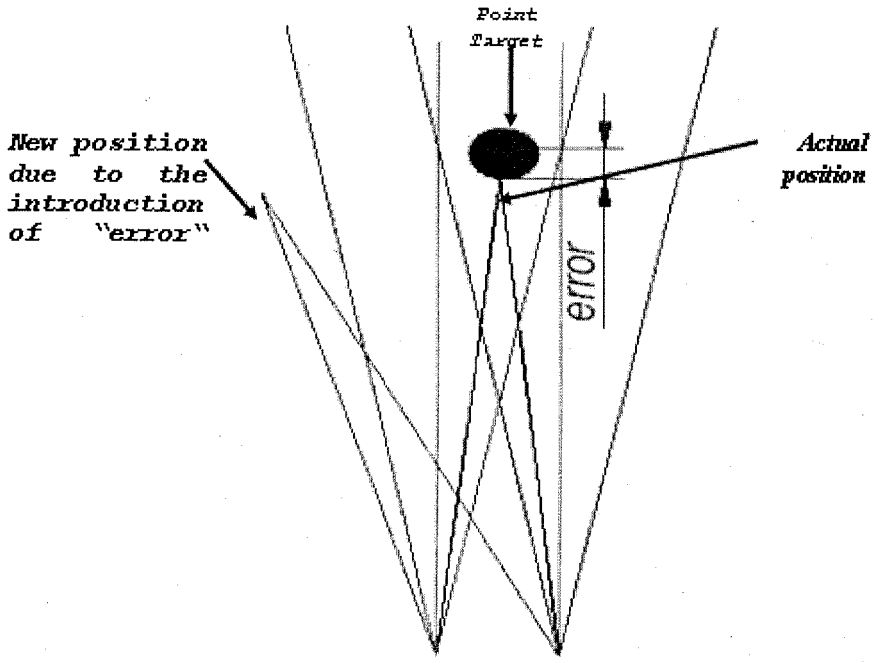

Fig. 3.2 Diagram illustrating the *geometric filter*

A candidate point selected as such is localized by triangulation and thereafter confirmed by implementing equation 2.4 as indicated earlier. An erroneous sonar return recorded by any of the two transducers due to, for example, weak signals would normally translate into a longer range value and as such will distort significantly the localization triangle thereby throwing off significantly a point localized within the visibility cone of any of the two transducers (See Figure 3.2). Theoretically therefore, this sensor will find it difficult to locate point targets with erroneous returns. In other words, this procedure filters out noisy data. The minimum range detectable by this model is given by:-

$(d/2)G \cot(\hat{a}/2) = 41\text{cm}. \ldots\ldots\ldots\ldots\ldots$ *(3.1*

This value in any case, is close to the minimum range of the standard Polaroid 6500 module; (30 cm). The implementation of this procedure as an embedded software was given the name *geometric filter.* Obviously, just two transducers can select and confirm a candidate point target. However, since the long term vision of this system is also to identify and localize short line segments, the triplet remains the best choice. The localization algorithm therefore has 7 possible ways of selecting a candidate point – noting that case 5 is excluded.

For the purpose of locating the closest point, it was decided not to scrutinize data beyond the second echo detected by each of the transducers. However, it would not be wise to rush to a conclusion that each transducer of the sonar triplet should be programmed to detect only two echoes. A third or fourth (or more) echo may carry hidden information on the target in question that is yet to be discovered. We can therefore summarize all the possible candidate point targets of the triplet as shown in Fig. 3.3. A localization code was subsequently developed taking into consideration all these facts. A flow chart of the algorithm implemented is illustrated on Appendix B. It can be seen from the flow chart that attention was focused essentially on identifying the edges of a rectangular target.

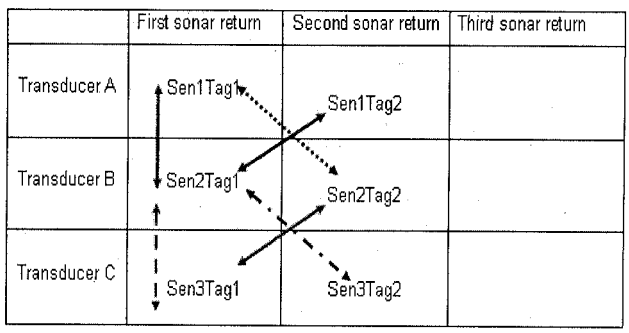

Fig. 3.3. Selecting candidate points

3.2 Localization tests with the monaural sonar ranging triplet

The first test (*Linear Data Consistency Test*, Fig. 3.4) that was carried out was to determine the accuracy as well as the consistency or repeatability of localizing an edge *(conveniently chosen to be an edge of a rectangular box- or a rectangular edge)* along the *width of view* and a range along the Y–axis extending from 100 to 300cm. A measurement interval of 5cm in the X-direction and 100cm in the y-direction were adopted for this test. The second test (*Edge Data Consistency Test* – Fig. 3.5) was done to ascertain whether a point target *(conveniently chosen to be the edge of a rectangular box- or a rectangular edge)* would maintain consistent data irrespective of its orientation. This test is important because the system is expected to localize a point target in a random manner. Beginning with 15°, an angular increment of the same value was maintained. The Y-interval was again maintained 100cm in the range between 100 and 250cm. These tests were in effect, calibration tests that should normally be done for any instrument system.

At this juncture, it is important for us to highlight the precision of the entire test system. The measurements tools (rulers, chalk markers, general purpose measuring tape, chalk board protractor) that were used had a precision of at least 5mm for linear measurement and 1.5° for angular measurement. The horizontal and vertical straightness of each transducer was just over 1mm per 50mm length. A rectangular target was used for all the tests. The three sonar transducers are supposed to be on a straight line but the alignment in both the vertical and horizontal direction was not better than 2mm per 50mm. The transducers were positioned with the aid of rulers and markers each with a precision of approximately 1.5mm.

3.3 Observations

The data obtained for the *linear data* and *angular consistency* test were tabulated as shown in Appendix C. According to this data, the maximum errors associated with the X and Y coordinates (***X_error and Y_error***) are – 8.0cm and 2.22 cm respectively. The corresponding mean errors and standard deviations are 3.64, 2.13, 1.72 and 0.48 respectively. A chart illustrating the error pattern of the range considered is shown on Fig. 3.6. The charts suggest a fair level of consistency in the errors recorded. However, in the second part of the ranging triplet, that is, between the centreline and third sensor, the *X_error* is lower and appears to be more consistent than within the first range (0 – 15cm).

Turning our attention to the angular consistency test of Fig. 3.5., the overall picture of the error pattern is also presented in Fig. 3.7. The maximum errors associated with the X and Y coordinates are – 7.56 cm and 2.39 cm respectively. The corresponding mean errors and standard deviations are 3.41, 2.64 and 1.45 and 0.66 respectively. Taking into consideration the fact that the precision of our experimental system is 0.5cm, we can conclude that the *mean errors* associated with both coordinates of the ranging triplet is **3.5cm** and ***1.5cm*** respec-

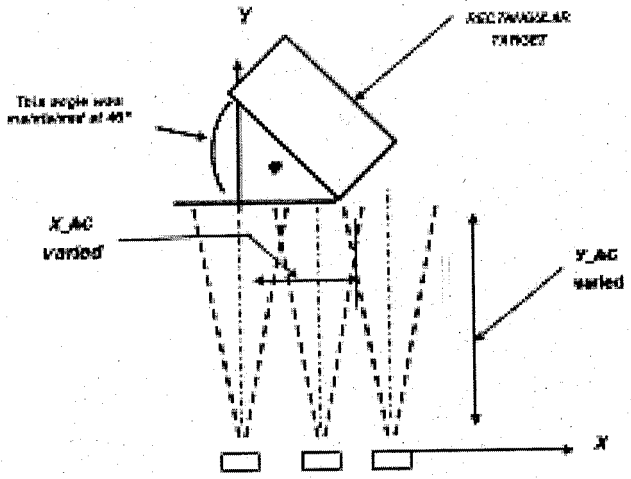

Fig. 3.4 Linear Data Consistency Test

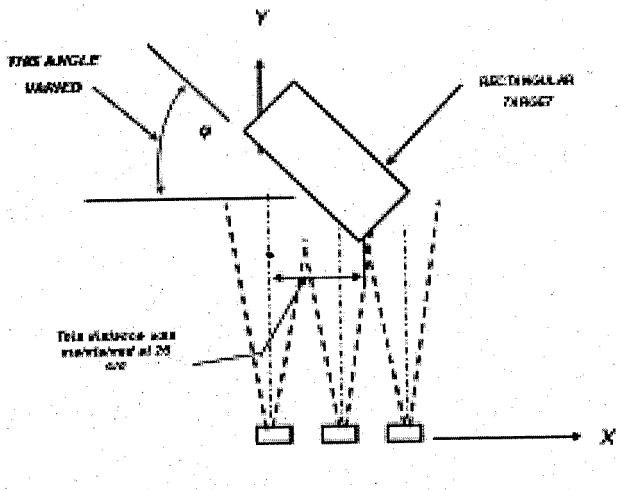

Fig. 3.5 . Edge or Angular Data Consistency Test

tively. By the same logic, the corresponding X and *Y standard deviations of the errors* are **2.5** and ***0.5cm*** respectively. Another important observation in both tests is that the Y-errors are basically positive (overestimation) while the X-errors are basically negative or underestimation. Furthermore, the data seems to suggests that errors are minimal when the orientation of an edge is 90°.

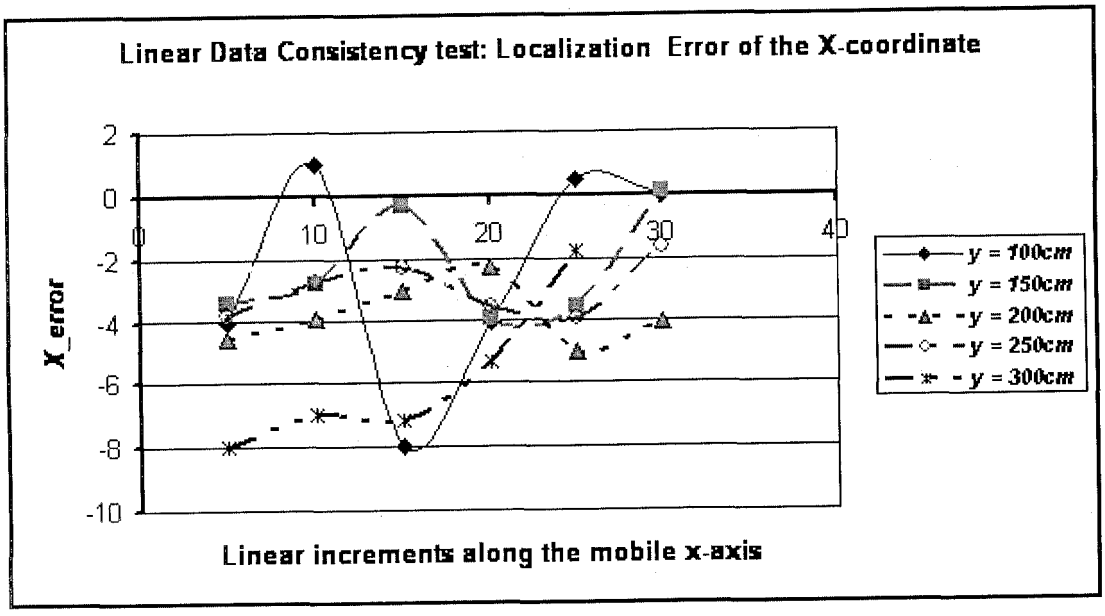

a)

Fig. 3.6 (a). Linear data Consistency test; error distribution

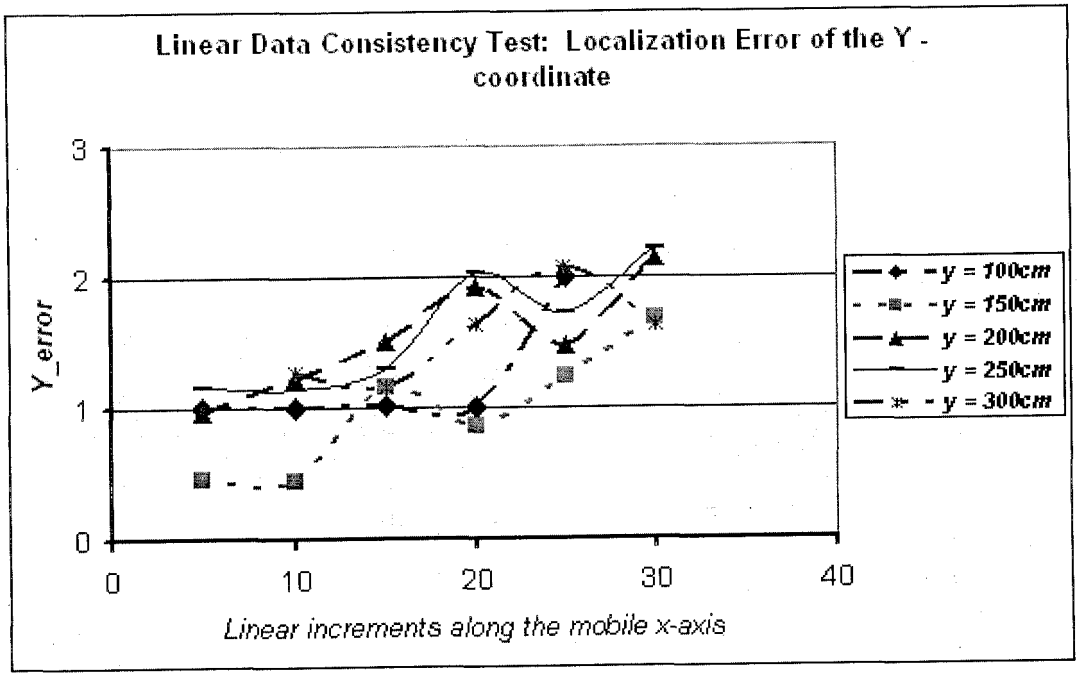

b)

Fig. 3.6(b). Linear data Consistency test; error distribution

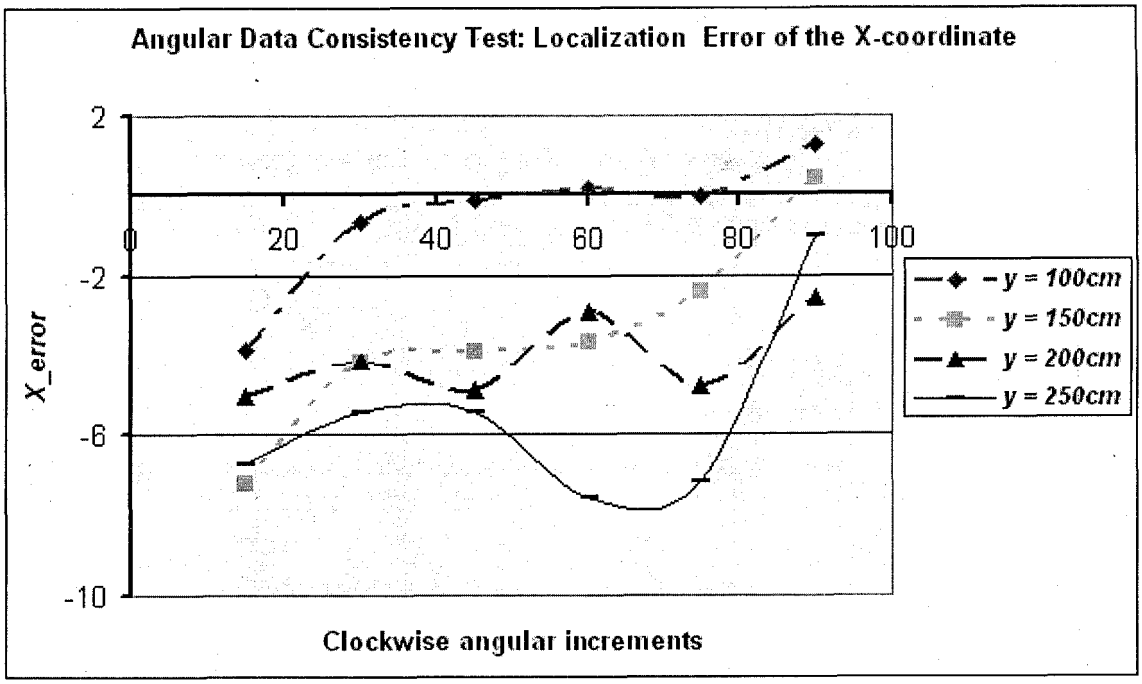

a)

Fig 3.7(a). Angular Data Consistency test, error distribution

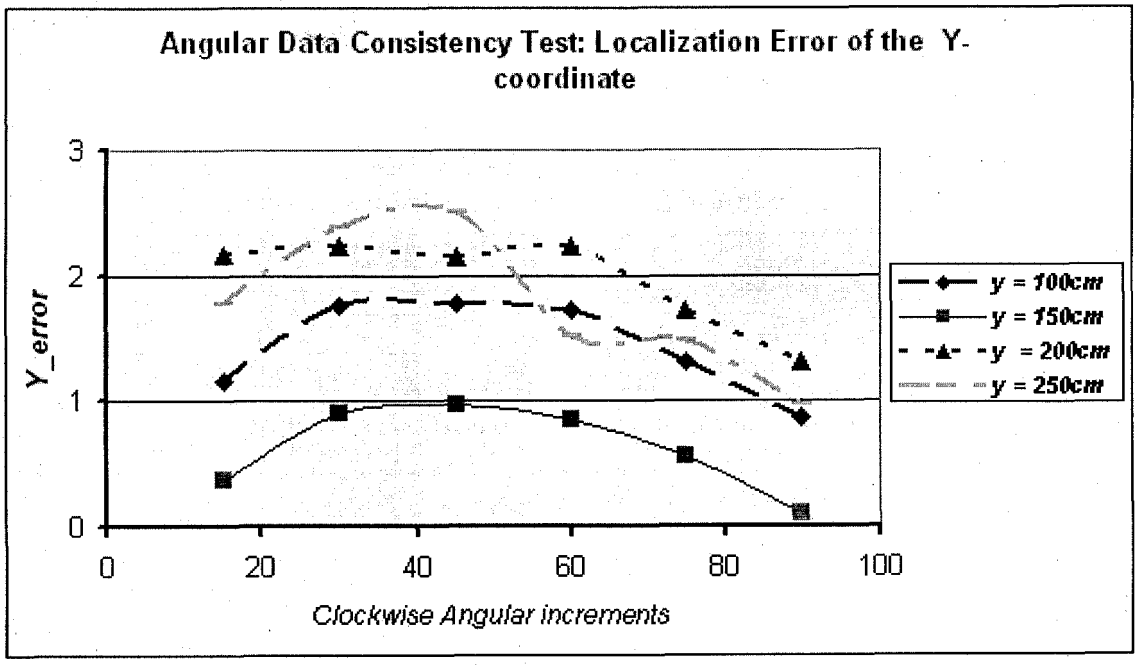

b)

Fig 3.7(b). Angular Data Consistency test, error distribution

3.4 Discussions

Evidently, autonomous navigation in an unknown 2D space could be greatly hampered if the heading of a target is not known within an error bound of at most 5°. From what has been observed so far, this ranging system (without any calibration) can be used to localize point targets if a precision on both the x and y axes of about 6cm is satisfactory. In other words, a rectangular target with a breadth of at least 70cm can be localized satisfactorily, speak-

ing within the context of 5° maximum heading precision.

However, our concern here is the localization of small mobile robots whose maximum length is less than 50cm. Does this suggest that this method cannot be applied to such robots? Not necessarily! First of all, we must point out that at its best, this ranging triplet can localize a point target within an error bound of less than 1cm. Moreover, the one-sided nature of the errors (*especially X_errors*) suggests that their sources are more systematic than random. In other words, we observed an error quarto-ellipse (Fig 3.8) instead of an error ellipse. These errors can be easily traced to the selection of candidate points. Considering the range in question (40cm to 550cm) as well as the spatial separation of the transducers, the maximum absolute separation to qualify a pair of returns as a candidate point can be estimated to be just below 2.5cm. Sticking on to this value however, could introduce significant errors because such a wide separation could also be due to weak energy sonar returns. As a matter of fact, the maximum separation chosen should reduce as the range increases since there is a greater likelihood of recording weak signals.

Another possible reason could be that the epicentre of reflected energy does not always coincide spatially with the point target causing the reflection. Besides, it has already been pointed out that the simple beam model is far from being an ideal inverted symmetrical expanding spherical cone.

For these reasons, the localization software was carefully reviewed (*or calibrated*) taking into consideration these observations. As a result, the Intelligent (TOF) sonar ranging triplet was able to localize with a precision of approximately 2cm (See Fig3.8 and data in appendix C). This value is quite reasonable because a better precision is hardly obtained even when ranging perpendicular target. because of reasons such as variations in temperature/humidity as well as some inherent hardware timing problems associated with the time of flight sonars, or in short, when working with poor quality sonars.

This is also an indication that a precisely built triplet operating with a carefully thought localization software could lead to a precision of less than 1.0cm. However, it is doubtful whether a precision of less 0.7cm (7mm) is obtainable with the Polaroid TOF sonar system because the wavelength of the ultrasonic sound associated with this system is about 7mm. Hence, the very fact that we have a high chance of achieving a precision of 1cm indicates that we are on the right track towards achieving an instant or *real time* localization of a point target with the Intelligent monaural sonar ranging triplet.

4. CONCLUSIONS AND SUGGESTIONS

The following conclusions can be drawn from this investigation: -

1. The monaural sonar sensor model proposed will localize a *point target* in 2D space with a precision of less than 2cm if both hard and software are carefully developed.
2. The same system can be used to discriminate between concave, convex and plane targets. Indeed, the same system can be used to localize short profiles or line segments

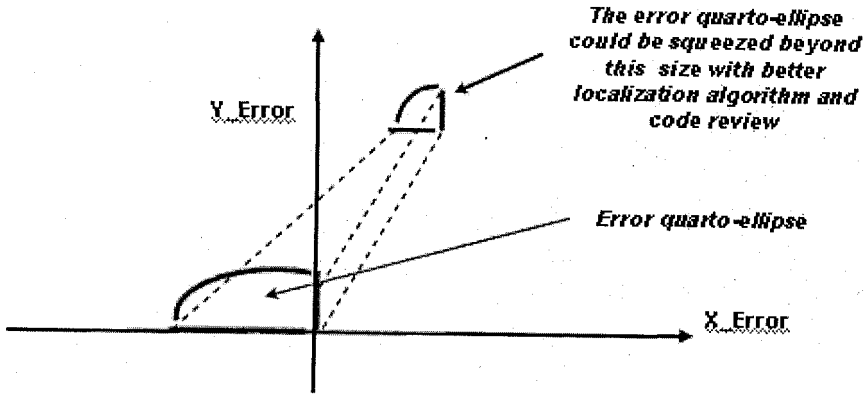

Fig. 3.8 Narrowing of the error *quarto*-ellipse as a result of calibration

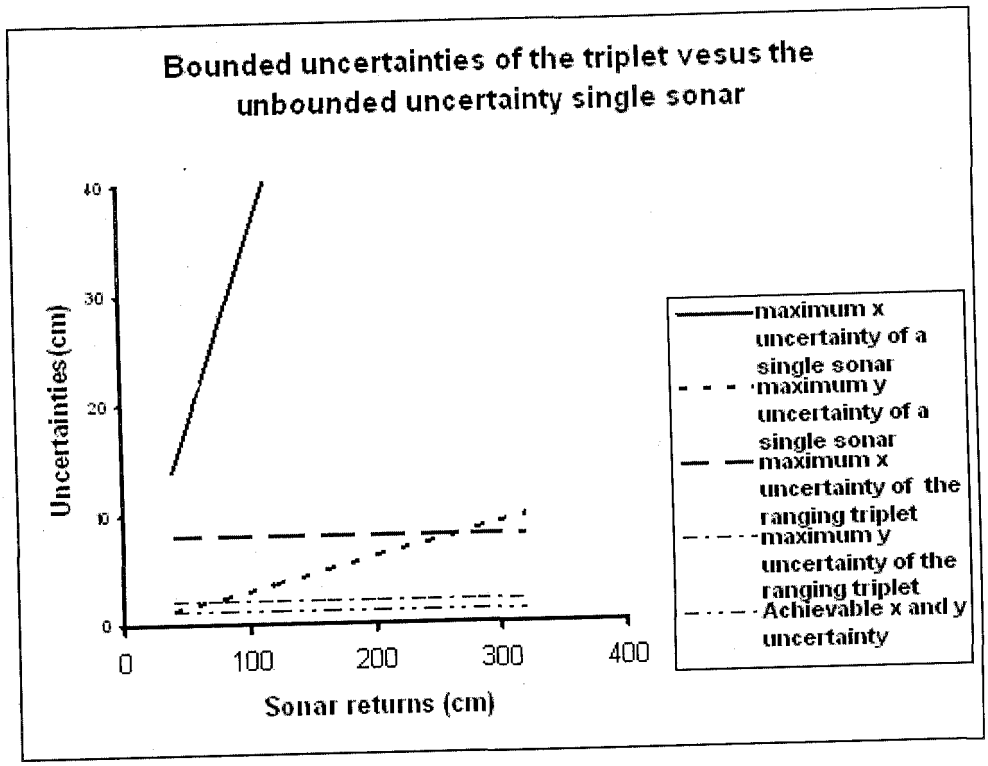

Fig 4.1 The underlining advantage of using a ranging triplet

corresponding to these geometric forms.

3. The consistent and relatively high underestimation of the X coordinate of the uncalibrated sensor suggests that the geometry associated with monaural sonar is neither conic nor symmetric as illustrated in Fig 1.1 .

A graphic illustration of the primary advantage of using a triplet as opposed to a single sonar transducer is illustrated by Fig. 4.1. We observe that when just a single sonar transducer is used in the single echo mode, the maximum X and Y uncertainties increase with the distance ranged and are boundless. The uncertainty associated with the X axis is more than ten times that of the y axis for the visibility angle in question i.e. 20°. Fig 4.1 also tells us that a rudimentary monaural ranging triplet bounds the X and Y uncertainty to values between 0 and 8cm and 0 and 2 cm respectively and that the attainment of a unified uncertainty bound between 0 and 1cm is feasible.

Accordingly, it is being suggested that the characteristics of the triplet arranged on an arc be investigation and it performance compared with a collinear triplet. It is also important that this work is confirmed with well aligned high quality monaural sonars modules. The localization algorithm may also be developed using probabilistic tools. Furthermore, this investigation has also exposed a hypothesis that the epicentre of reflected sound energy does not always coincide with the point initiating the reflection. This conclusion should be of interest to sound wave propagation physicists.

ACKNOWLEDGMENTS

I am heavily indebted to the University of Applied Sciences Ravensburg – Weingarten, Germany, for giving me the opportunity to carry out this research in one of its outstanding lab – the Autonomous Robotics Systems (ARS) Lab. The same feeling of gratitude is being extended to Prof Dr. Klaus Schilling who directed and provided the funding for this research. I am also thanking in a special way the entire Autonomous Robotics Systems team of the academic year 2002/2003, and in particular Mr. Radu Barza for his invaluable contributions and suggestions throughout this research work.

REFERENCES

1. **Gisbert Lawistzky, Wendelin Feiten, Marcus Möller.** (1995) Sonar sensing for low cost indoor mobility. Robotics and Autonomous Systems 14 : 149 –157.

2. **John J. Leonard and Hugh F. Durrant Whyte**(1992) Directed sonar sensing for mobile robot navigation. Kluver Academic Publishers, Massachusetts, USA: p. 18.

3. **Kenneth D. Harris and Michael Reece** (1998). Experimental modelling of time-of-flight sonar. Robotics and Autonomous Systems 14: 33 – 42.

4. **R . Kuc and M.W. Siegel,**(1987). Physically based simulation model for acoustic sensor robot navigation. IEEE Transactions on Pattern Analysis and Machine Intelligence 9 - 1987, 766 -778.

5. **Wijk, O. and Christensen, H.I.** (2000) Localization and navigation of a robot using natural point landmarks extracted from sonar data. Robotics and Autonomous Systems. 31:(1-2): Elsevier Science BV, Netherlands. pp.31 - 42.

Received: 06/01/2005
Accepted: 18/09/2005

APPENDIX A-Experiments with a collinear sonar triplet

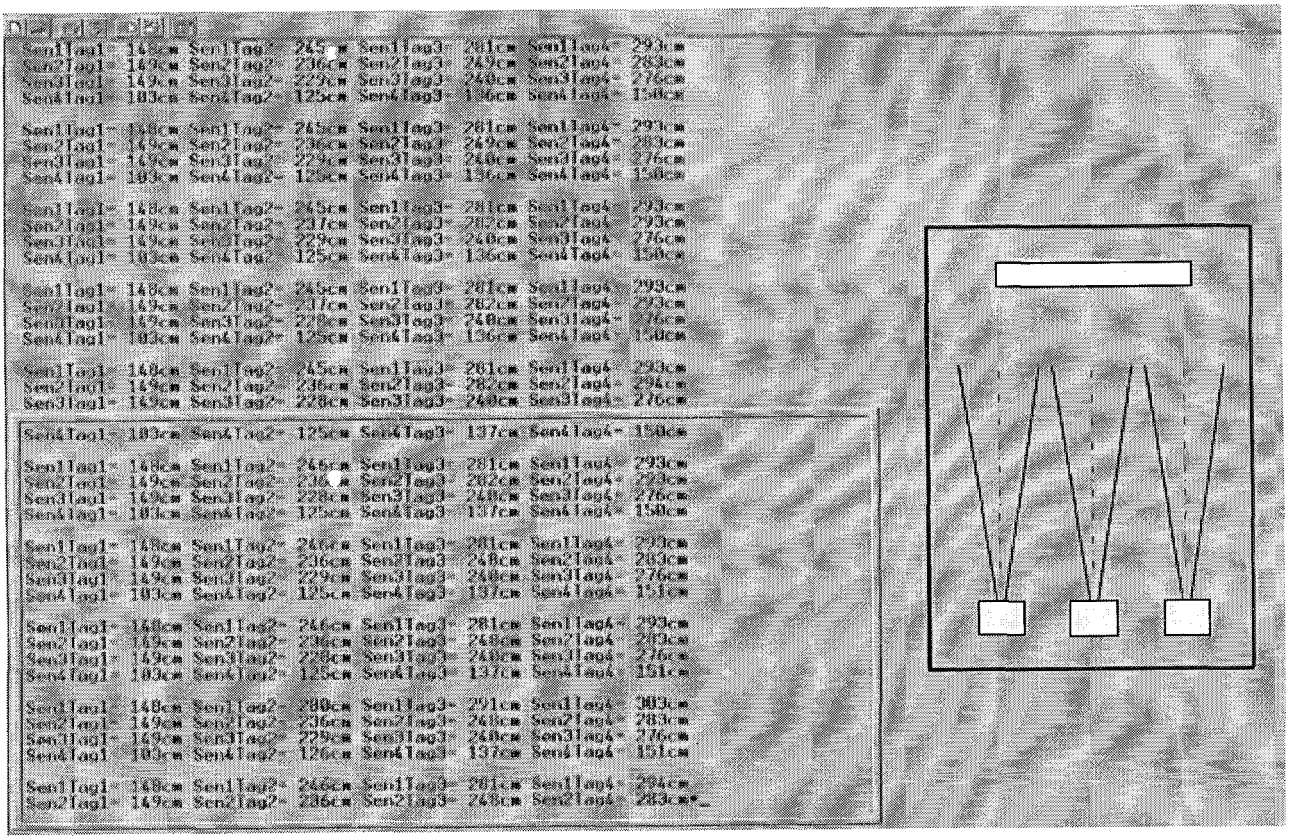

Fig.A1 Parallel plane

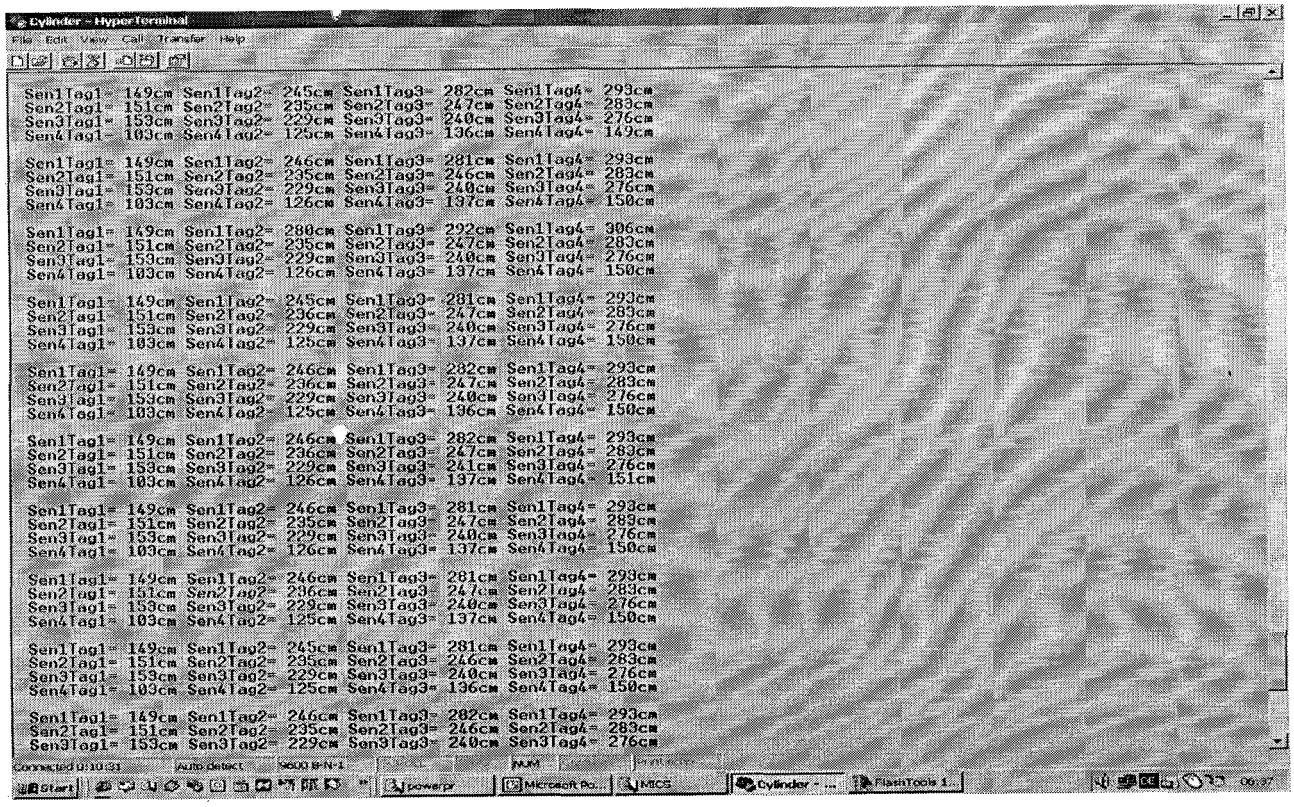

Fig. A2. Inclined plane – less than10°

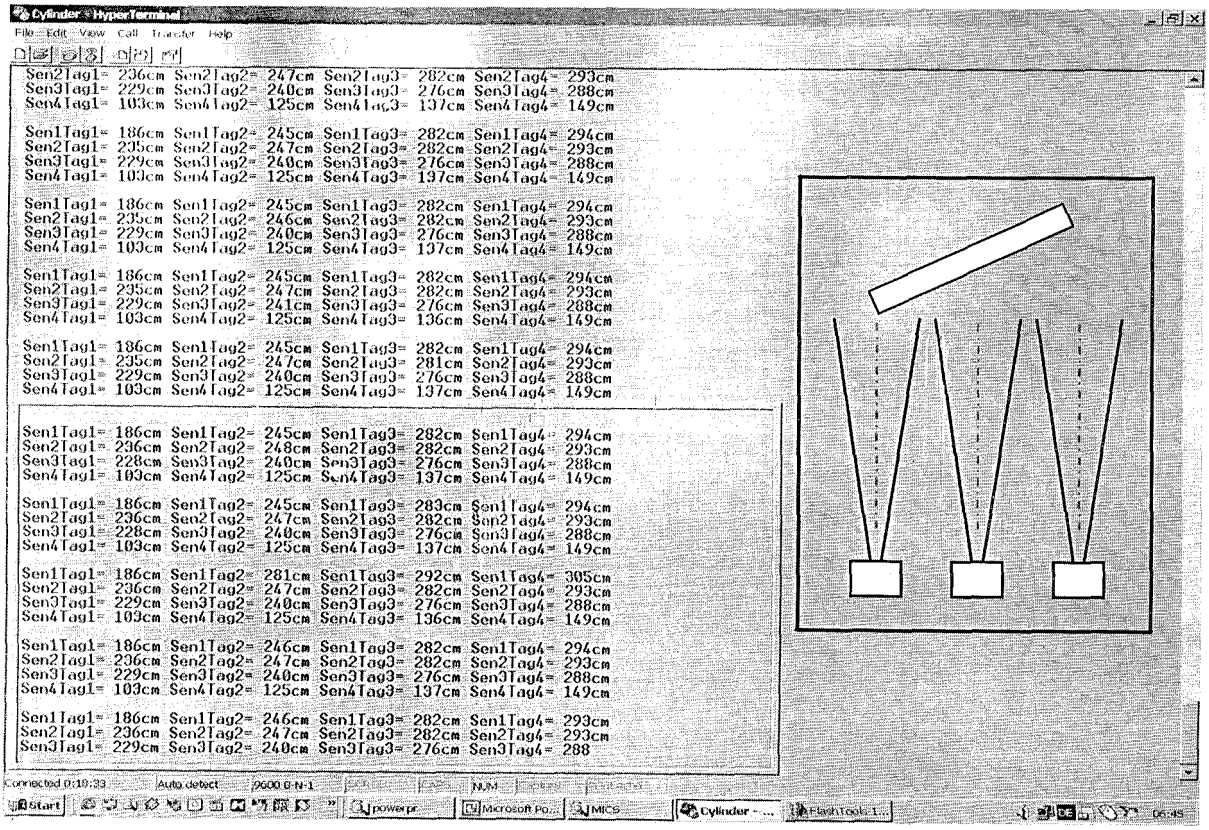

Fig. **A3.** Inclined plane – more than10°

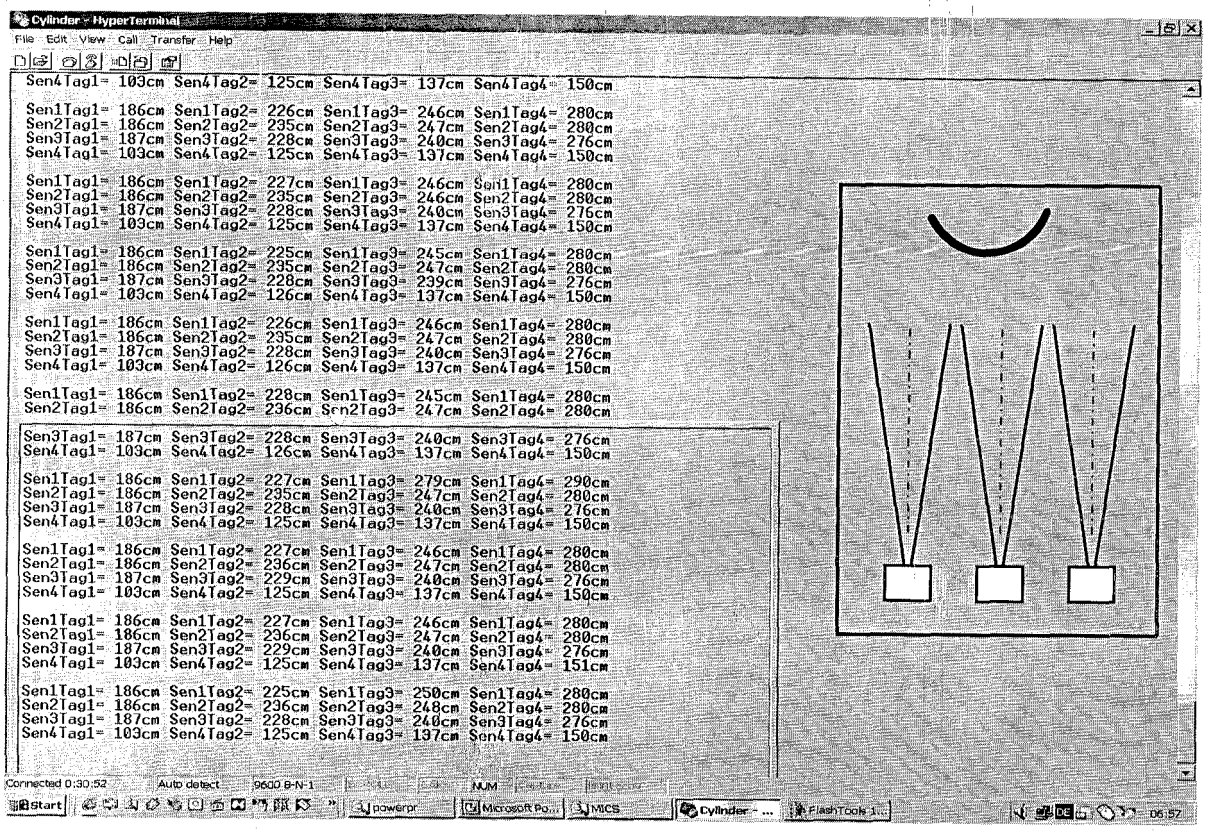

Fig. **A4.** Convex Cylindrical Surface

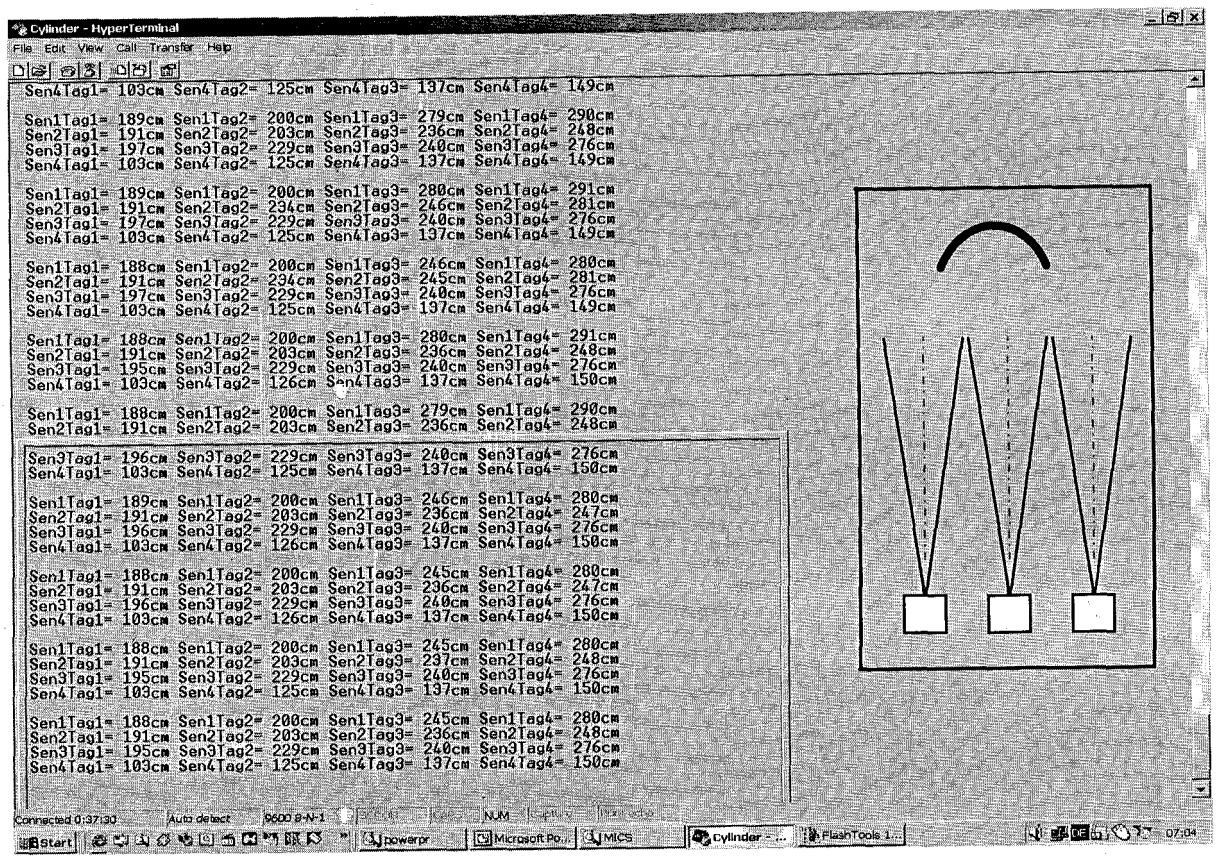

Fig. A5. Concave Cylindrical Surface

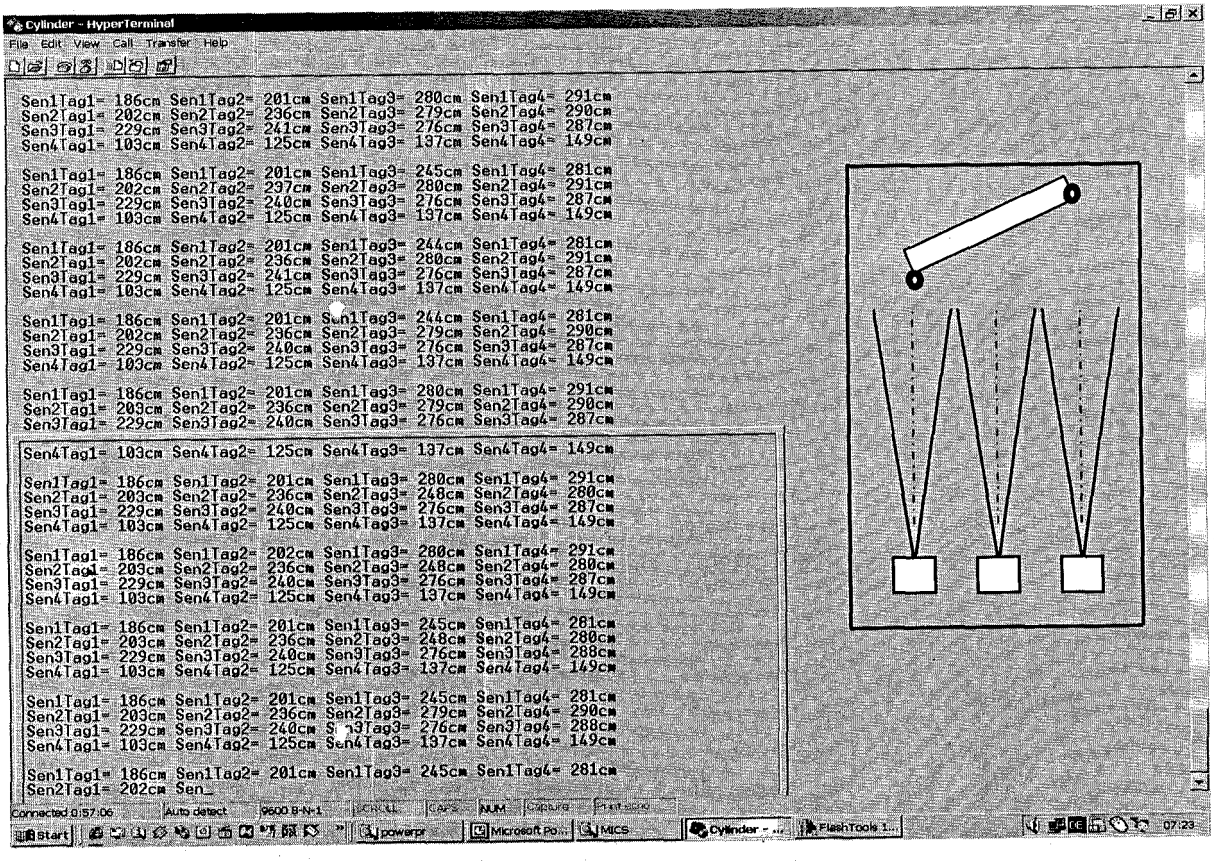

Fig. A6. Inclined plane – more than 10° with edges made "visible" with sand paper

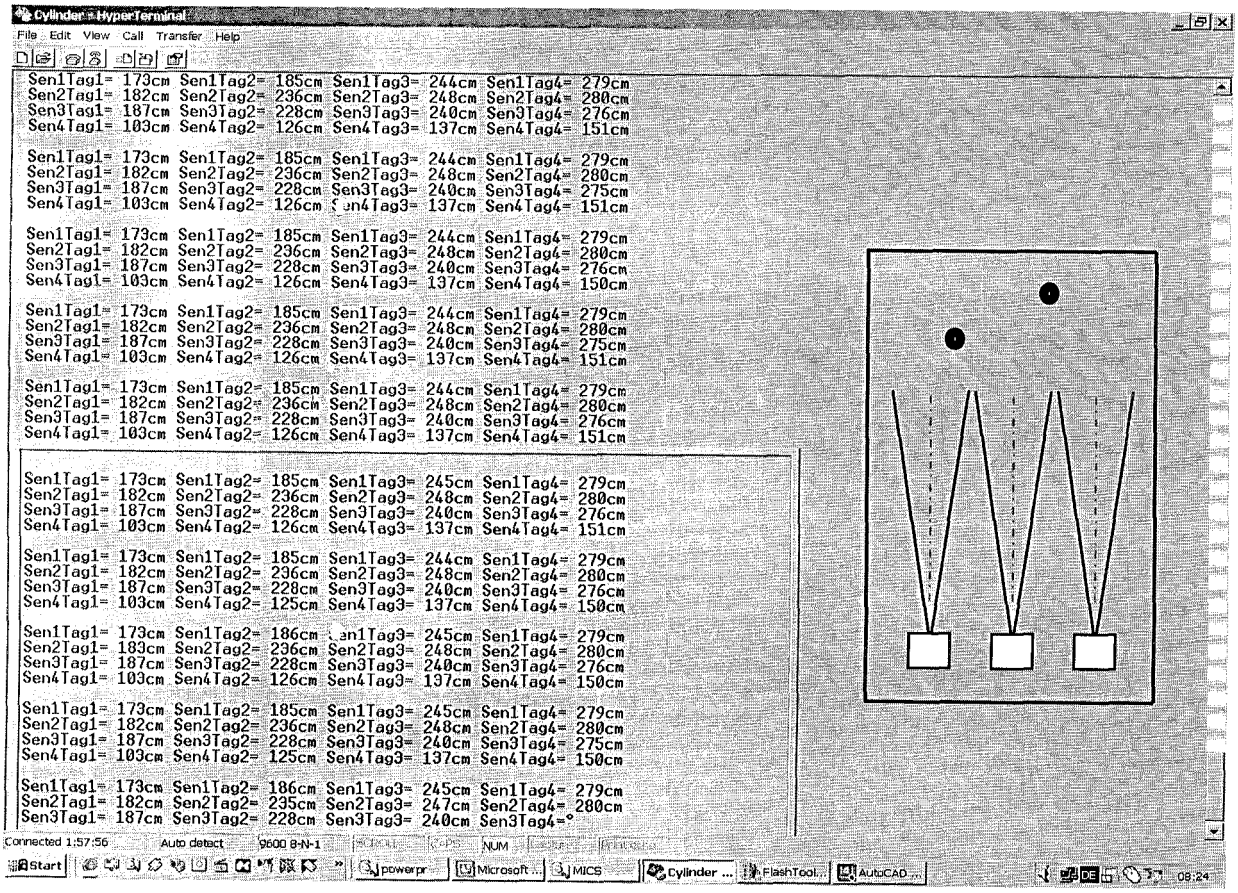

Fig. A7. Data for two isolated points of each of radius 15mm

APPENDIX B

FLOW CHART FOR THE POINT TARGET LOCALIZATION ALGORITHM

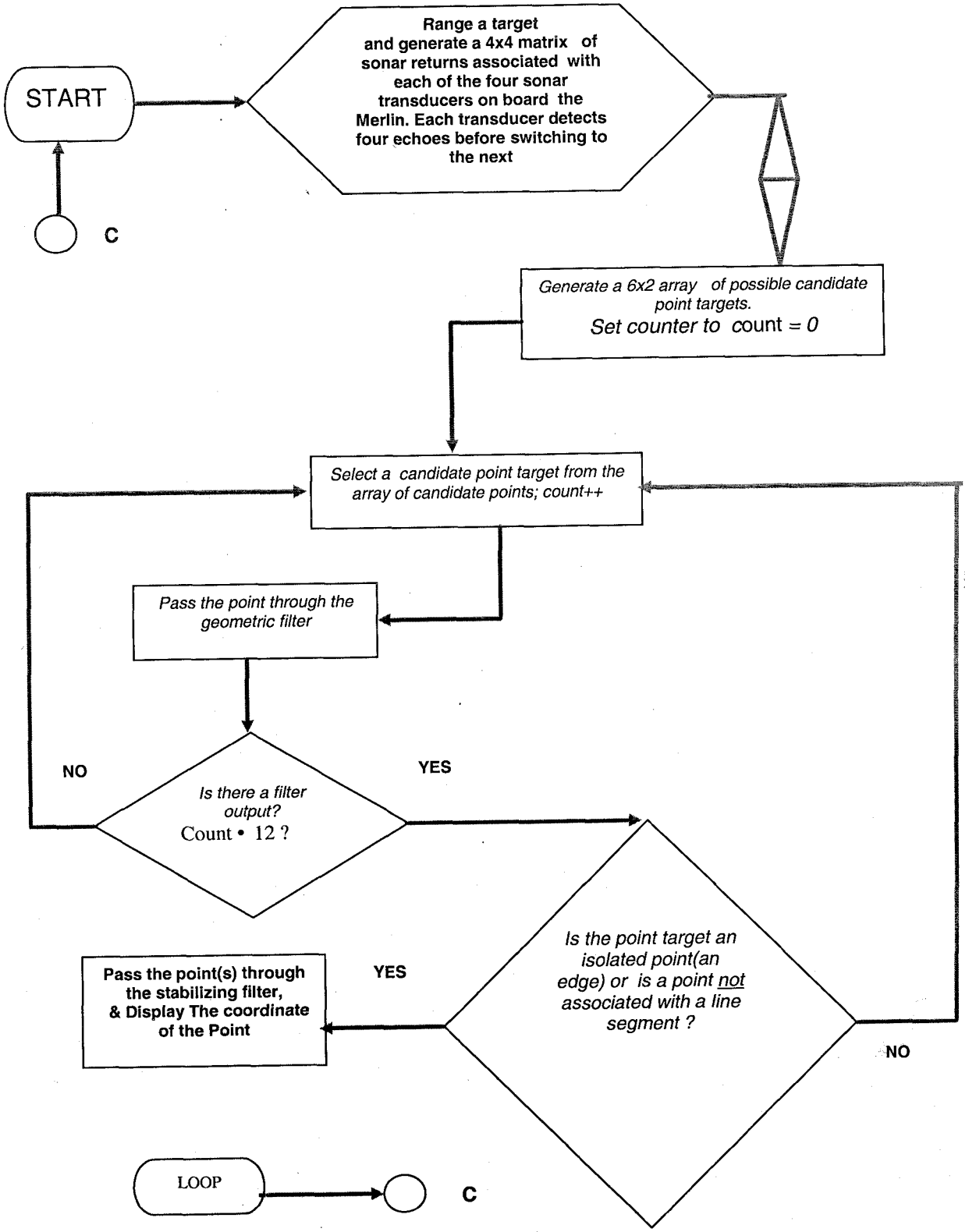

APPENDIX C-Tests with the sonar ranging triplet system

The table below is the data recorded for the ***Linear Data Consistency test.*** The legend associated with this table is as follows:-

X_ac = Actual x coordinate of an edge.
Y_ac = Actual y coordinate of an edge.
X_ms = x coordinate estimated by the triplet ranger
Y_ms = y coordinate estimated by the triplet ranger
X_error = X_ms - X_ac
Y_error = Y_ms - Y_ac

The maximum x and y errors are in italic.

Table C1

X_ac	*Y_ac*	*Theta_ac*	*X_ms*	*Y_ms*	*X_error*	*Y_error*
5.00	100.00	45.00	1.00	101.00	-4.00	1.00
10.00	100.00	45.00	11.00	101.00	1.00	1.00
15.00	100.00	60.00	7.03	101.01	-7.97	1.01
20.00	100.00	45.00	16 .00	101.00	-4.00	1.00
25.00	100.00	45.00	25.50	102.00	0.50	2.00
30.00	100.00	45.00	ND	ND	ND	
5.00	150.00	45.00	1.58	150.46	-3.42	0.46
10.00	150.00	45.00	7.23	150.44	-2.77	0.44
15.00	150.00	45.00	14.67	151.15	-0.33	1.15
20.00	150.00	45.00	16.07	150.86	-3.93	0.86
25.00	150.00	45.00	21.46	151.23	-3.54	1.23
30.00	150.00	45.00	30.13	151.69	0.13	1.69
5.00	200.00	45.00	0.39	200.97	-4.61	0.97
10.00	200.00	45.00	6.12	201.22	-3.88	1.22
15.00	200.00	45.00	11.99	201.52	-3.01	1.52
20.00	200.00	45.00	17.70	201.92	-2.30	1.92
25.00	200.00	45.00	19.95	201.49	-5.05	1.49
30.00	200.00	45.00	25.95	202.14	-4.05	2.14
5.00	250.00	45.00	1.20	251.15	-3.80	1.15
10.00	250.00	45.00	7.27	251.13	-2.73	1.13
15.00	250.00	45.00	12.75	251.30	-2.25	1.30
20.00	250.00	45.00	16.46	252.03	-3.54	2.03
25.00	250.00	45.00	21.11	251.73	-3.89	1.73
30.00	250.00	45.00	28.33	252.22	-1.67	***2.22***
5.00	300.00	45.00	ND	ND	ND	ND
10.00	300.00	45.00	2.00	301.27	***-8.00***	1.27
15.00	300.00	45.00	8.00	301.15	-7.00	1.15
20.00	300.00	45.00	12.81	301.65	-7.19	1.65
25.00	300.00	45.00	19.64	302.09	-5.36	2.09
30.00	300.00	45.00	28.26	301.64	-1.74	1.64
MEAN					**-3.51cm**	**1.37cm**
STANDARD DEVIATION					**2.32cm**	**0.48cm**

The next table shows the data recorded for the *Angular Consistency Test.* The legend is the same except for ö which represents the orientation of the "orthogonal edge" used.

Table C2

• (°)	X_ac	Y_ac	X_ms	Y_ms	X_error	Y_error
15.00	25.00	100.00	21.17	101.16	-3.83	1.16
30.00	25.00	100.00	24.31	101.76	-0.69	1.76
45.00	25.00	100.00	24.89	101.78	-0.11	1.78
60.00	25.00	100.00	25.18	101.72	0.18	1.72
75.00	25.00	100.00	24.98	101.31	-0.02	1.31
90.00	25.00	100.00	26.27	100.87	1.27	0.87
15.00	25.00	150.00	17.77	150.37	-7.23	0.37
30.00	25.00	150.00	20.86	150.90	-4.14	0.90
45.00	25.00	150.00	21.09	150.97	-3.91	0.97
60.00	25.00	150.00	21.34	150.85	-3.66	0.85
75.00	25.00	150.00	22.57	150.56	-2.43	0.56
90.00	25.00	150.00	25.40	150.10	0.40	0.10
15.00	25.00	200.00	19.96	202.16	-5.04	2.16
30.00	25.00	200.00	20.86	202.23	-4.14	2.23
45.00	25.00	200.00	20.10	202.15	-4.90	2.15
60.00	25.00	200.00	22.08	202.24	-2.92	2.24
75.00	25.00	200.00	20.20	201.73	-4.80	1.73
90.00	25.00	200.00	22.45	201.31	-2.55	1.31
15.00	25.00	250.00	18.27	251.78	-6.73	1.78
30.00	25.00	250.00	19.55	252.39	-5.45	2.39
45.00	25.00	250.00	19.56	252.50	-5.44	***2.50***
60.00	25.00	250.00	17.44	251.52	***-7.56***	1.52
75.00	25.00	250.00	17.82	251.49	-7.18	1.49
90.00	25.00	250.00	24.00	250.97	-1.00	0.97
MEAN					**-3.41**	**1.45**
STANDARD DEVIATION					**2.64**	**0.66**

Table C3. Errors associated with X and Y coordinates after calibration

x_ac	y_ac	x_ms	y_ms	X_error	Y_error
8.00	100.00	7.89	101.02	-0.11	1.02
15.00	145.00	13.40	146.70	-1.60	1.70
8.00	195.00	5.16	195.70	-2.84	0.70
19.00	245.00	16.49	247.68	-2.51	2.68
12.00	295.00	10.11	296.82	-1.89	1.82
6.50	100.00	4.42	100.82	-2.08	0.82
13.50	145.00	12.17	146.60	-1.33	1.60
12.00	195.00	10.02	196.16	-1.98	1.16
24.50	245.00	23.38	246.91	-1.12	1.91
14.00	295.00	12.31	296.47	-1.69	1.47
MEAN				**-1.72**	**1.49**
STANDARD DEVIATION				**0.76**	**0.59**